Progress In Electromagnetics Research M, Vol. 80, 93–102, 2019

Design and Development of Compact Reconfigurable Tri-Stopband Bandstop Filter Using Hexagonal Metamaterial Cells for Wireless Applications

Khelil Fertas[1, *], Farid Ghanem[2], Mouloud Challal[3], and Rabia Aksas[1]

Abstract—In this paper, a compact reconfigurable tri-band bandstop filter (BSF) with sharp-rejection and high selectivity is presented. The proposed filter is based on a 50 Ohms microstrip feed line, six hexagonal metamaterial cells (HMCs) with different sizes and switches. The structure of the filter has seven different modes of operation characterized. A good agreement between the simulated and measured results is obtained. The results indicate that the proposed filter design, with overall size of $0.28\lambda g \times 0.17\lambda g$, is a good candidate for multiservice radios applications.

1. INTRODUCTION

In recent years, the demand for compact microstrip filters is growing due to the newly expanding microwave and mobile communication systems [1–4]. In order to reduce the complexity and overall volume of such systems, compact and flexible structures like reconfigurable filters are used [5–10]. One of the advantages of these filters is their aptitude to reconfigure in frequency, consequently, reducing the area allocated to the various radio frequency (RF) front ends for different wireless communication standards incorporated into the final product.

In the literature, various types of reconfigurable bandstop filters were proposed [11–13]. Therefore, the use of compact reconfigurable filters has become increasingly important. Diverse methods were used to obtain reconfigurable filters using diodes [14, 15] or based on electrostatic MEMS [16]. Some structures, each corresponding to a mode of operation with ideal switches, were realized as well in literature [17]. Moreover, several studies have been conducted to use the metamaterial in microwaves structures in order to change their characteristics [18–20] particularly in filters structures [21–23].

In this paper, a novel compact reconfigurable tri-stopband BSF with sharp-rejection and high selectivity is designed, fabricated, and measured. The filter structure, printed on a Rogers RT5870 dielectric substrate with a relative dielectric constant of 2.33, thickness of 0.508 mm, and loss tangent of 0.0012, is composed of a 50 Ohms microstrip feed line and six hexagonal metamaterial cells (HMCs) with different sizes and switches. The proposed filter has seven different modes of operation characterized, mainly, into three types: single, dual, and triple stopbands. The simulation and measurement results are presented and discussed. The proposed reconfigurable tri-stopband BSF has acceptable results indicating that this type of filter is well suited for multiservice radios applications.

Received 23 October 2018, Accepted 26 March 2019, Scheduled 8 April 2019

* Corresponding author: Khelil Fertas (khelil.fertas@g.enp.edu.dz).

[1] Ecole Nationale Polytechnique, Electronics Department, El-Harrach, Algiers, Algeria. [2] Telecom Product Direction, R&D&I, Brandt Group, Cevital Industry Pole, Garidi II, Algiers, Algeria. [3] Signals and Systems Laboratory, Department of Electronics, Institute of Electrical and Electronic Engineering, University M'hamed Bougara of Boumerdes, Boumerdes, Algeria.

2. FILTER DESIGN AND CONFIGURATION

2.1. Hexagonal-Shaped Metamaterial Cell

A hexagon-shaped metamaterial cell (HMC) can be derived from a simple structure of the H-SRR used by [24]. The H-SRR and HMC geometries are described in Figures 1(a)–(b), respectively. In Figure 1(b), the HMC consists of one ring, which is the same as the outer ring of the conventional H-SRR with two arms mounted inside cell. This modification increases the electrical length which permits to achieve a miniaturization. In this case, the HMC dimensions are optimized in order to reject three distinct frequencies that are 3.6 GHz, next 5.2 GHz, and finally 5.8 GHz. The HMC is designed in a Rogers RT 5870 board with a thickness of 0.508 mm, dielectric constant of 2.33, and loss tangent of 0.0012. Table 1 presents the physical dimensions of the structure for three distinct frequencies, abbreviated by cell 1, cell 2, and cell 3.

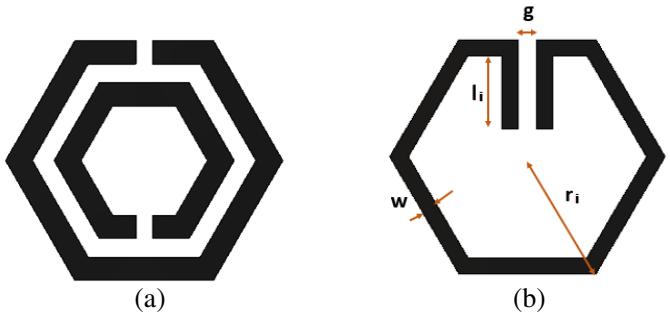

Figure 1. Layouts of (a) H-SRR and (b) HMC.

The two most important parameters in metamaterial cells modeling are actual effective permeability (μ) and tangent magnetic loss ($\tan\delta$). This loss is calculated by using the imaginary part of the permeability characteristics according to the following equation: $\tan\delta = -\text{Imaginary}(\mu)/\text{Real}(\mu)$.

Figure 2 illustrates the negative real part permeability characteristics of the HMCs at the frequencies of 3.5 GHz, 5.2 GHz, and 5.8 GHz. The design and analysis of the real part of the permeability produced by the cells are performed using the full-wave electromagnetic simulators CST microwave studio. It is evident from Figure 2 that the metamaterial effects are obtained due to the HMCs structure that exhibits a negative real part of permeability properties with narrow frequency bands at real (μ) equal to zero (as shown by dashed line).

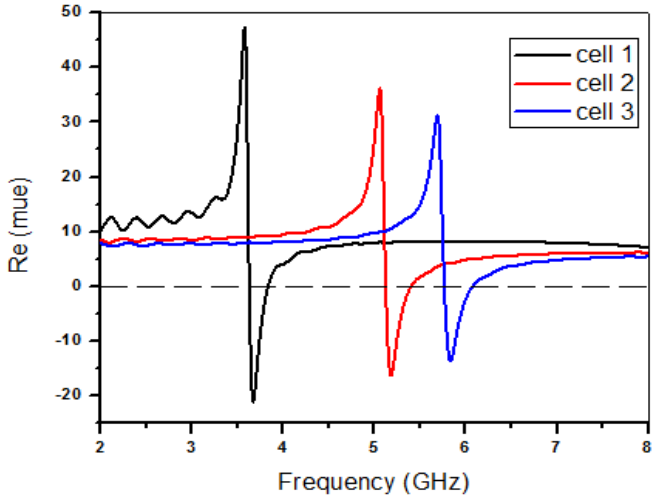

Figure 2. Real-parts of permeability for the three HMCs.

Table 1. Optimized parameters.

parameter	cell 1		cell 2		cell 3	
	$l1$	$r1$	$l2$	$r2$	$l3$	$r3$
value	3.1	4	2.1	3	1.8	2.8

2.2. Tri-Stopband BSF Configuration

The layout of the suggested tri-stopband BSF is displayed in Figure 3. The proposed structure consists of a 50 Ω microstrip line along with three pairs of HMCs of different sizes that are placed in cascade. The three pairs of HMCs are arranged so as to have good coupling with the feed line.

The filter dimensions are obtained and optimized using the CST software. Indeed, the initial dimensions were fixed as a first step, and then, according the aim of the work, they were optimized such that the structure provided three desired stopband frequencies.

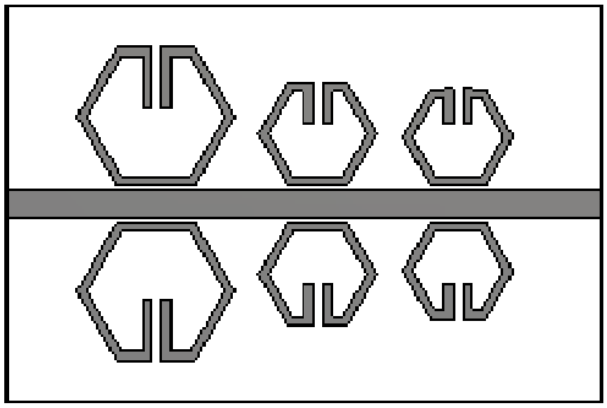

Figure 3. Geometry of the proposed tri-stopband without switches BSF.

The negative permeability of each pair of HMCs produces a magnetic coupling with the feed line that starts to operate at distinct frequencies, as shown in Figure 5. From Figure 5, it can be seen that the simulated structure behaves as BSF which rejects three distinct frequencies; the first one corresponds to 3.64 GHz with a rejection level close to −16 dB, and the two others correspond to 5.25 GHz and 5.8 GHz with rejection levels close to −22.1 dB and −23.5 dB, respectively. Besides, near 0 dB insertion loss outside these bands is obtained.

To investigate the behavior of the proposed filter with tri-stopband characteristics, an equivalent LC circuit model is proposed in Figure 4. In addition, each stopband can be modeled as a parallel LC resonance circuit. The equivalent capacitance C and inductance L can be calculated using Equation (1)

$$C = \frac{1}{2\pi Z(f_u - f_l)}, \quad L = \frac{1}{4\pi^2 f_0^2 C} \tag{1}$$

where f_l and f_u are lower and upper cutoff frequencies at −10 dB, and Z represents the input impedance of filter and can be obtained from the simulated results.

The lumped components are optimized and tuned using ADS software to obtain the stopbands. The simulated S-parameters from the equivalent circuit and full-wave simulation are compared, as shown in Figure 5. According to the comparison results, the provided circuit is applicative to the filter structure.

The current distribution of the simulated structure is presented in Figure 6. One can clearly see that the current remains mainly concentrated and distributed along the HMC. The coupling distance has a considerable effect on the filter. When decreasing this distance, the coupling between cells increases significantly and leads to shifting of the resonant frequency. The design is optimized such that the cells

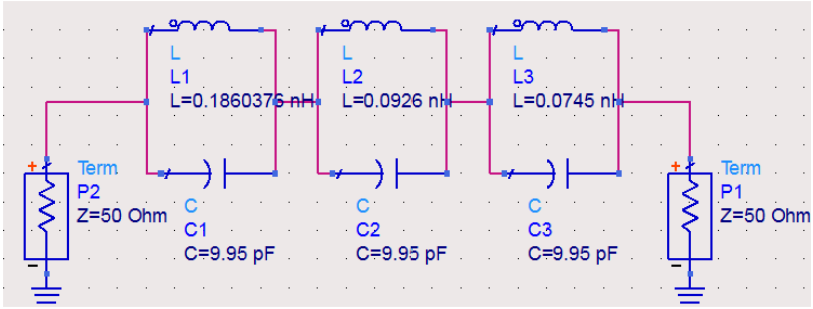

Figure 4. The LC resonant circuit model of proposed filter.

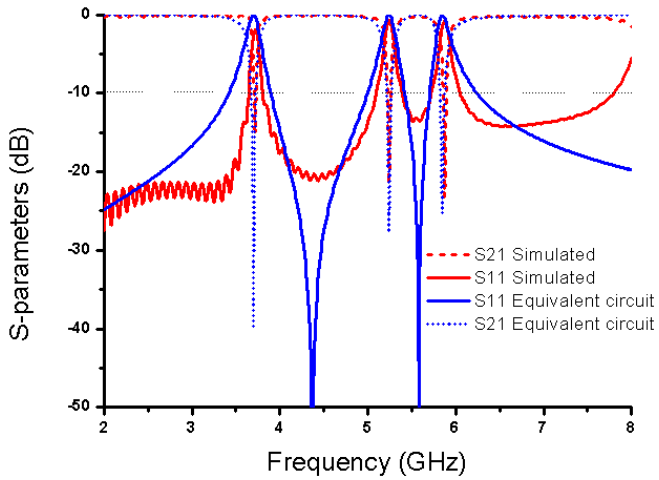

Figure 5. *S*-parameters of the proposed tri-stopband BSF.

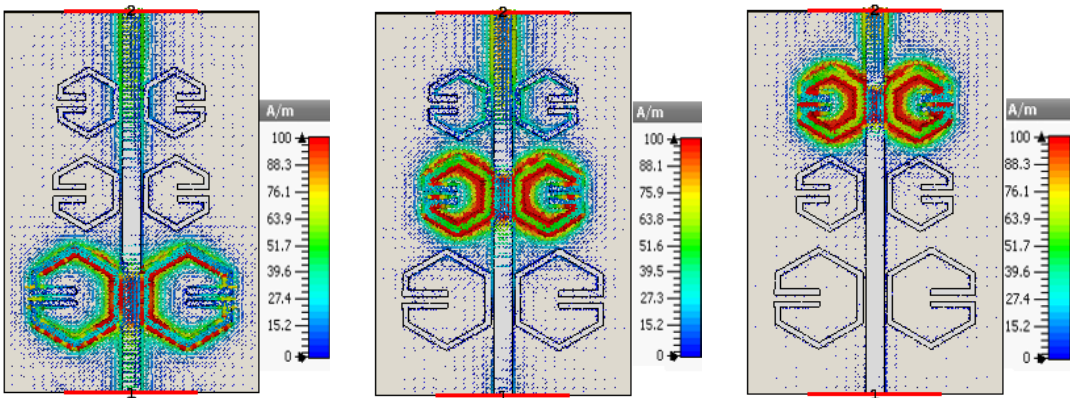

Figure 6. Current distribution (a) at 3.64 GHz, (b) at 5.25 GHz and (c) at 5.8 GHz.

work separately without coupling effect. This figure confirms the results obtained in the previous figure where each cell creates a stopband.

2.3. Switchable BSF Configuration

To achieve frequency reconfiguration, six switches are inserted into the gap between the two arms of each cell as shown in Figure 7. In order to validate the reconfiguration mechanism by means of switches,

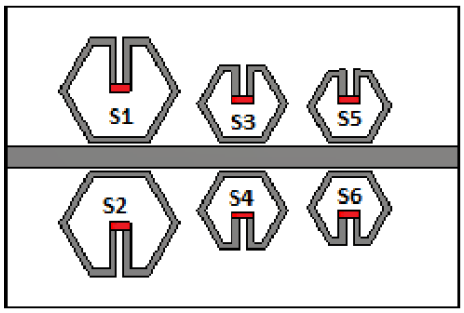

Figure 7. Geometry of the proposed tri-stopband BSF.

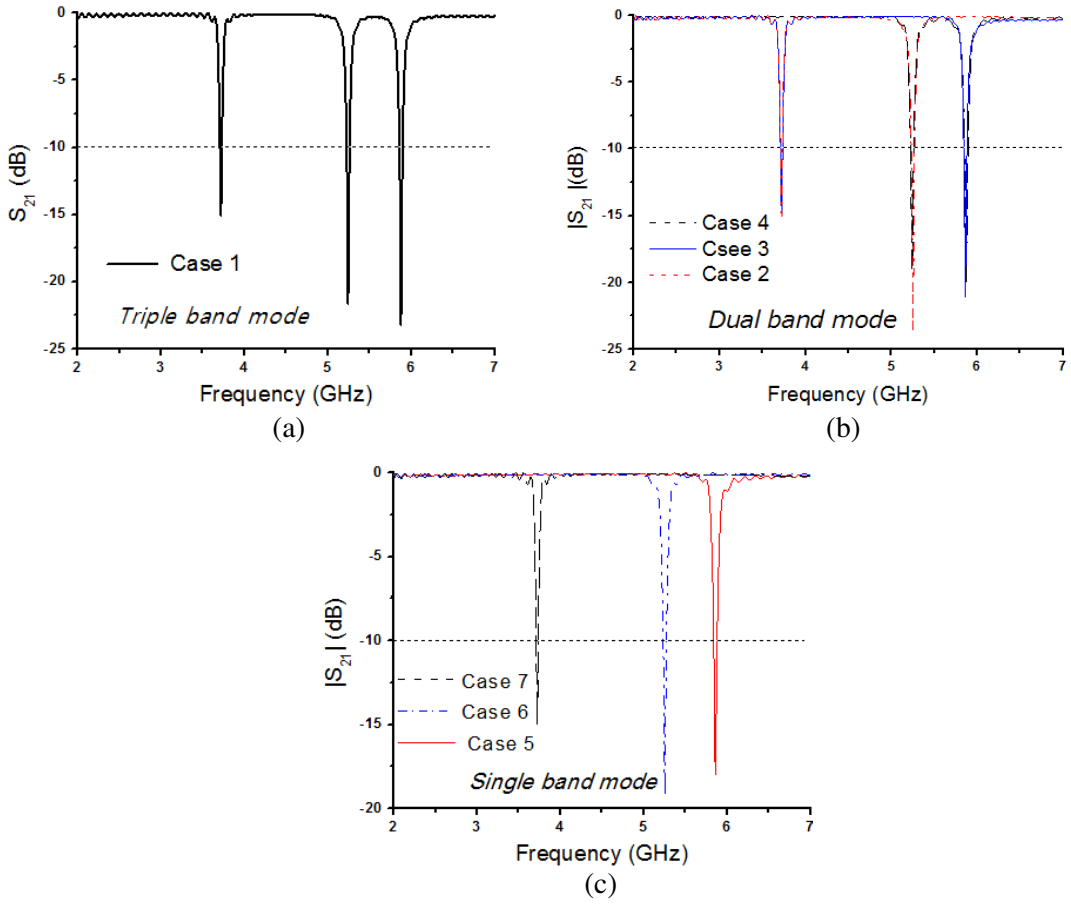

Figure 8. Simulated S_{21} magnitude of the proposed filter. (a) Triple band mode, (b) dual band mode and (c) single band mode.

the two operating states of the switch "ON/OFF" were modelled by the PRESENCE/ABSENCE of a perfect conductor strip of the same size as that of a real switch. The switch positions have been optimized to annul the operation bands when the latter is closed. The proposed reconfigurable filter has seven different modes of operation as revealed in Figure 8. As seen from Figure 8, if we deactivate each pair of HMCs, then the corresponding band of band-stop filter disappears without affecting the filter response of other frequencies.

An interesting property of metamaterial cell is its ability to concentrate electrostatic energy from the incident field in the regions where a capacity behavior is created. When an external magnetic field

is applied to HMC in "OFF state" of the switch, it induces a current flowing on the metallic inclusion and creates a resonant frequency which is inversely proportional to the electrical length. On the other hand, when the switch is "ON", a resonant frequency disappears because of the absence of current.

Different configurations of the switches for each operating state are summarized in Table 2.

Table 2. Configuration of switches for all cases.

Modes	S1&S2	S3&S4	S5&S6	Stopband frequency (GHz)
Case 1	OFF	OFF	OFF	3.5/5.2/5.8
Case 2	OFF	OFF	ON	3.5/5.2
Case 3	OFF	ON	OFF	3.5/5.8
Case 4	ON	OFF	OFF	5.2/5.8
Case 5	ON	ON	OFF	5.8
Case 6	ON	OFF	ON	5.2
Case 7	OFF	ON	ON	3.5

3. EXPERIMENTAL VALIDATION: RESULTS AND DISCUSSIONS

In order to practically demonstrate the effectiveness and advantages of the proposed configuration, several filters, each corresponding to a mode of operation with ideal switches, were realized and tested with an R&S®ZNB VNA. A photograph of one of the fabricated prototypes is displayed in Figure 9. The simulated and measured results are presented in Figure 10.

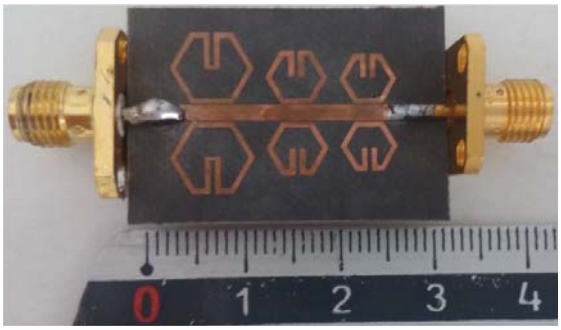

Figure 9. Photograph of one of the fabricated prototypes (case 4).

From Figure 10, a good agreement between simulated and measured results is achieved validating the reconfigurable behaviour in frequency. The stopband frequencies of the filter (case 1) were measured to be f_{s1} of 3.6 GHz, f_{s2} of 5.2 GHz, and f_{s3} of 5.8 GHz, with respective fractional bandwidths of 1.89%, 1.91%, and 1.82%. The small deviation between the measured and simulated results was, most probably, attributed to the dielectric substrate loss and the unpredicted tolerances in the fabrication and soldering of the connectors.

Usually, group delay is used to evaluate the phase response. Ideally, when the phase response is strictly linear, the group delay is constant. The measured group delay characteristic for one of the fabricated prototypes (case 1), shown in Figure 11, is approximately constant for the frequency range of the filter, and its variation is within 0.5 ns. In the rejection bands, the measured group delay shows fluctuations mainly because of the impedance mismatching , which is around 3.167 ns, 3.082 ns, and 4.1 ns, at 3.75 GHz, 5.18 GHz, and 5.91 GHz, respectively.

The performance comparison of the proposed reconfigurable tri-stopband BSF with those reported in literature is illustrated in Table 3. It can be seen that the proposed filter provides good performances in terms of high selectivity, very small FBW, and low insertion loss.

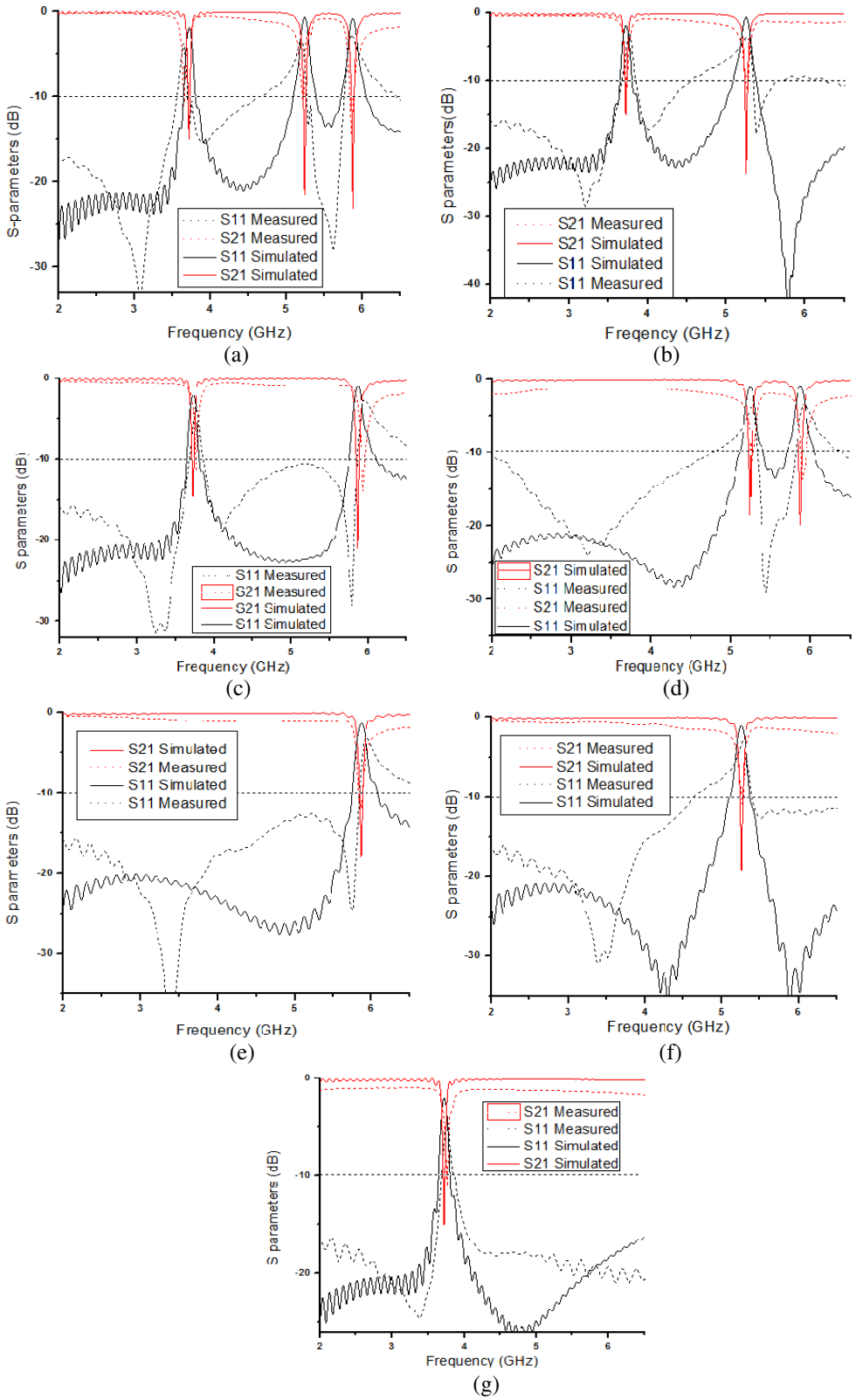

Figure 10. Simulated and measured S-parameters of the proposed filter for: (a) Case 1, (b) Case 2, (c) Case 3, (d) Case 4, (e) Case 5, (f) Case 6, (g) Case 7.

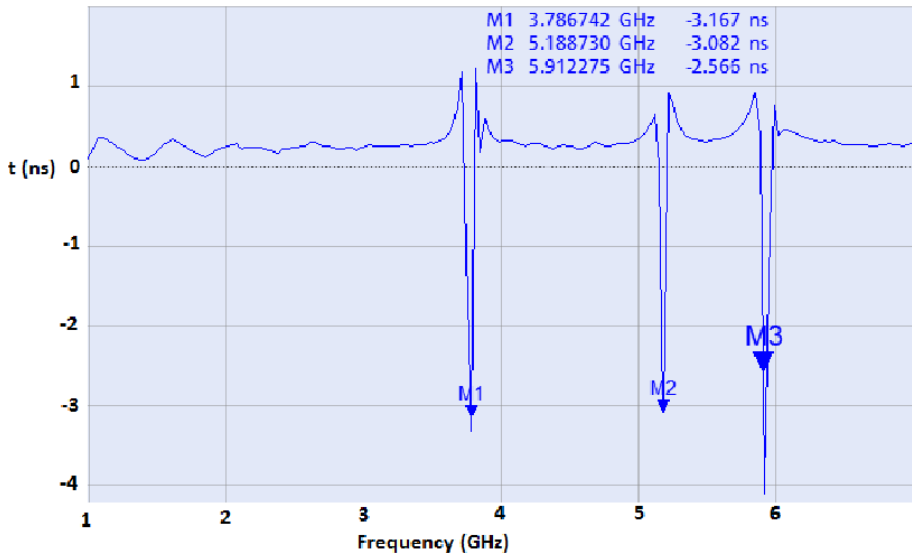

Figure 11. Measured group delay response of one of the fabricated prototypes (case 1).

Table 3. Comparison of performance characteristics with reported tri-stopband BSFs.

	[25]	[26]	[27]	This current work
Substrate ε_r/h (mm)	2.2/1.575	3.38/0.813	4.3/1.58	2.33/ 0.508
Stopband frequencies (GHz)	2.4/3.5/5.2	4/6.3/8.3	2.6/5.57	3.5/5.2/5.8
FBW (%)	4.2/ 2.9/ 4.5	40/ 39/24	> 40	1.89/1.91/1.82
IL (dB)	$-1.5/-2.54/-1.16$	> -1	$-0.47/-1.28$	$-1.5/-0.7/-0.6$
Total size ($\lambda g \times \lambda g$)	$0.21\lambda g \times 0.11\lambda g$	$0.37\lambda g \times 0.25\lambda g$	$0.41\lambda g \times 0.76\lambda g$	$0.28\lambda g \times 0.17\lambda g$
Reconfigurability	no	no	yes	yes

4. CONCLUSION

In this paper, a novel concept of a compact reconfigurable tri-stopband BSF with sharp-rejections using hexagonal metamaterial cells and switches has been designed, fabricated, and tested. The filter has seven different modes of operation characterized, mainly three types: single, dual, and triple stopbands. The stopband frequencies of the filter (case where all switches are taken OFF) have been measured and are 3.5 GHz, 5.2 GHz, and 5.8 GHz, with respective fractional bandwidths of 1.89%, 1.91%, and 1.82%. The measurement results compared to the simulation ones have shown a good agreement validating the reconfigurable behaviour in frequency. The most application areas of this proposed filter topology are wireless communications, MIMO communication, and RF circuit.

ACKNOWLEDGMENT

The authors express their thanks to Dr. A. Mansoul, Development Centre of Advanced Technologies (CDTA), Algiers, Algeria and to the responsible of Signals and Systems Laboratory (LSS), Institute of Electrical and Electronic Engineering, University M'Hamed Bougara of Boumerdes, Boumerdes, Algeria, for providing support and assistance to perform simulations by using software and, for the help during the fabrication and measurement of the proposed compact reconfigurable tri-stopband BSF prototype.

REFERENCES

1. Gao, X.-K., H. M. Lee, and S.-P. Gao, "A robust parameter design of wide band DGS filter for common-mode noise mitigation in high-speed electronics," *IEEE Trans. on Electromagn. Compat.*, Vol. 59, No. 6, 1735–1740, 2017.
2. Boutedjar, A., "Design of compact reconfigurable broadband band-stop filter based on a low-pass filter using half circle DGS resonator and multi-layer technique," *Progress In Electromagnetics Research C*, Vol. 71, 91–100, 2017.
3. Jadhav, J. B. and P. J. Deore, "A compact planar ultra-wideband bandpass filter with multiple resonant and defected ground structure," *AEU — Intern. J. of Electron. and Commun.*, Vol. 81, 31–36, 2017.
4. Lalbakhsh, A., G. Karimi, and F. Sabaghi, "Triple mode spiral wideband bandpass filter using symmetric dual-line coupling," *E. Lett.*, 2017.
5. Arnold, C., J. Parlebas, and T. Zwick, "Reconfigurable waveguide filter with variable bandwidth and center frequency," *IEEE Trans. on Microw. Theor. and Techn.*, Vol. 62, No. 8, 1663–1670, 2014.
6. Cheng, T. and K.-W. Tam, "A wideband bandpass filter with reconfigurable bandwidth based on cross-shaped resonator," *IEEE MWCL*, 2017.
7. Cho, Y.-H. and G. M. Rebeiz, "0.73–1.03-GHz tunable bandpass filter with a reconfigurable 2/3/4-pole response," *IEEE Trans. on Microw. Theor. and Techn.*, Vol. 62, No. 2, 290–296, 2014.
8. Feng, W., Y. Shang, et al., "Multifunctional reconfigurable filter using transversal signal-interaction concepts," *IEEE MWCL*, 2017.
9. Kheir, M., T. Kröger, and M. Höft, "A new class of highly-miniaturized reconfigurable UWB filters for multi-band multi-standard transceiver architectures," *IEEE Access*, Vol. 5, 1714–1723, 2017.
10. Boutejdar, A., et al., "A miniature 5.2-GHz bandstop microstrip filter using multilayer-technique and coupled octagonal defected ground structure," *Microwave and Optical Technology Letters*, Vol. 51, No. 12, 2810–2813, 2009.
11. Lee, K., T.-H. Lee, et al., "Reconfigurable dual-stopband filters with reduced number of couplings between a transmission line and resonators," *IEEE MWCL*, Vol. 25, No. 2, 106–108, 2015.
12. Esmaeili, M. and J. Bornemann, "Novel tunable bandstop resonators in SIW technology and their application to a dual-bandstop filter with one tunable stopband," *IEEE MWCL*, Vol. 27, No. 1, 40–42, 2017.
13. Wong, K. W., R. R. Mansour, and G. Weale, "Reconfigurable bandstop and bandpass filters with wideband balun using IPD technology for frequency agile applications," *IEEE Trans. on Comput., Packag. and Manuf. Tech.*, Vol. 7, No. 4, 610–620, 2017.
14. Tsai, H.-J., B.-C. Huang, et al., "A reconfigurable bandpass filter based on a varactor-perturbed, T-shaped dual-mode resonator," *IEEE MWCL*, Vol. 24, No. 5, 297–299, 2014.
15. Boutejdar, A., "Design of 5 GHz-compact reconfigurable DGS-bandpass filter using varactor-diode device and coupling matrix technique, " *Microwave and Optical Technology Letters*, Vol. 58, No. 2, 2016.
16. Han, Z., K. Kohno, et al., "Tunable terahertz filter and modulator based on electrostatic MEMS reconfigurable SRR array," *IEEE J. of Selec. Top. in Quan. Electron.*, Vol. 21, No. 4, 114–122, 2015.
17. Mansoul, A., "Switchable multiband slot antenna for 2.4, 3.5 and 5.2 GHz applications," *MOTL*, Vol. 59, No. 11, 2903–2907, 2017.
18. Anuja, K., "A survey on metamaterial based microstrip patch antenna," *Wirel. Commun.*, Vol. 9, No. 3, 54–60, 2017.
19. Semmar, B., R. Aksas, et al., "Numerical determination of permittivity and permeability tensors of a dielectric metamaterial composed of an infinite number of split ring resonators," *WPC*, Vol. 83, No. 4, 2925–2947, 2015.

20. Yu, A., F. Yang, and A. Z. Elsherbeni, "A dual band circularly polarized ring antenna based on composite right and left handed metamaterials," *Progress In Electromagnetics Research*, Vol. 78, 73–81, 2008.
21. Wang, R.-L., J.-F. Wang, et al., "Dual-band suspended stripline filter based on metamaterials," *2017 International Applied Computational Electromagnetics Society Symposium (ACES)*, 1–2, IEEE, 2017.
22. Bhaskar, M., J. Jasmi, and T. Mathew, "Microstrip bandstop filters based on hexagonal complementary split ring resonators," *2015 Fifth International Conference on Advances in Computing and Communications (ICACC)*, Sept. 2–4, 2015.
23. Mohammed, M. and B. Suwailam, "Numerical study of bandstop filters based on slotted complementary split ring resonators," *Proc. Second International Conf. on TAEECE*, 34–37, 2014.
24. Saktioto, T., R. F. Syahputra, et al., "GHz frequency filtering source using hexagonal metamaterial splitting ring resonators," *MOTL*, Vol. 59, No. 6, 1337–1340, 2017.
25. Janković, N., R. Geschke, and V. Crnojević-Bengin, "Compact tri-band bandpass and bandstop filters based on Hilbert-fork resonators," *IEEE MWCL*, Vol. 23, No. 6, 282–284, 2013.
26. Boutejdar, A. and S. D. Bennani, "Design and fabrication of tri-stopband bandstop filters using cascaded and multi-armed methods," *Adv. Electromagn.*, Vol. 6, No. 3, 18–24, 2017.
27. Nachouane, H., A. Najid, et al., "A switchable bandstop-to-bandpass reconfigurable filter for cognitive radio applications," *Intern. J. of Microw. and Wirel. Technol.*, Vol. 9, No. 4, 765–772, 2017.